Journal of Inorganic and Organometallic Polymers and Materials (2023) 33:1507–1516
https://doi.org/10.1007/s10904-023-02551-w

RESEARCH

The In-Vitro Effect of Silver and Zinc Oxide Nanoparticles on Fluoride Release and Microhardness of a Resin-Modified Glass Ionomer Cement

Dalal AlMatar[1] · Shaikha AlSanousi[1] · Jasim Ahmed[2] · Syed Saad Bin Qasim[1]

Received: 27 December 2022 / Accepted: 18 January 2023 / Published online: 27 March 2023

Abstract
Reinforcement of nanoparticles into existing restorative biomaterials in dentistry is an area of interest. The aim of the current investigation was to incorporate silver nanoparticles (SNP) and zinc oxide nanoparticles (ZnONP) into a commercially available resin-modified glass ionomer cement (RMGIC). Their effects on the fluoride (F-) release from RMGIC were also investigated over a period of 14-days. Nanoparticles were incorporated at a loading concentration of 5 wt%, either individually or in a combination of both. Scanning electron microscopy (SEM), Fourier Transform infrared spectroscopy (FTIR), Nanocomputerized tomography (NanoCT), and the Vickers microhardness tester were used to examine the specimens. The fluoride release was analyzed by high performance liquid chromatography (HPLC). Data were analysed using ANOVA and Tukey's test. RMGIC containing 5% ZnONP and 5% SNP + 5% ZnONP showed significant alterations in the surface ultrastructure with pores being evident in the surface. Fluoride release in parts per million (ppm) was highest in the 5% SNP and 5% ZnO-NP incorporated RMGIC compared to the control group and 5% SNP-incorporated RMGIC. RMGIC, as well as change in color observed in the 5% SNP incorporated RMGIC.

Keywords Color stability · Fluoride · Microhardness · Nanoparticles · Resin modified glass ionomer cement · Silver · Zinc Oxide

1 Introduction

The first glass ionomer cements (GIC) were introduced in the late 1970s. Since its invention, advances in restorative dentistry have produced several variants of this material [1]. Resin modified glass ionomer cements (RMGICs) have gained popularity amongst dentists as the material of choice when treating pediatric patients, due to their preventive characteristics, ease of placement, and aesthetics [2, 3]. RMGICs contain not only the basic formulation of conventional GIC, like fluoroaluminosilicate glass and an aqueous solution of polyacrylic acid, but they have added water-soluble monomers like 2-hydroxyethyl methacrylate (HEMA) or bisphenol A-glycidyl methacrylate (Bis-GMA), which may or may not be grafted onto the polyacrylic acid [4]. The RMGICs have some advantages over the conventional GICs. Specifically, they allow a longer working time, control of the photochemical curing process by the clinician, and a rapid hardening of the surface of the cement. Therefore, the photochemical reactions decrease the early sensitivity to moisture and the dehydration associated with the early stage of the acid-base reaction in the conventional GIC [5].

Nevertheless, there are certain physiochemical and biomechanical hurdles with this restorative material that still need to be addressed. Additionally, interest has been further developed in using RMGICs as dental bonding agents [6]. An in vitro study suggested that the bond strength of RMGIC is inferior to resin composites; however, it is adequate for bonding orthodontic brackets [7]. The availability of free monomers in RMGIC also renders them less biocompatible as compared to conventional GIC [8]. Hence, investigators across the globe are putting more effort into studying the effects of different additives on RMGIC.

✉ Syed Saad Bin Qasim
sayed.binqasim@ku.edu.kw

Jasim Ahmed
Jaahmed@kisr.edu.kw

[1] Department of Bioclinical Sciences, Faculty of Dentistry, Kuwait University, Safat, Kuwait

[2] Environment and Life Sciences Research Center, Kuwait Institute for Scientific Research, Safat, Kuwait

Advancement in nanotechnology has broadened its therapeutic applications to dentistry. Metallic nanoparticles have been extensively studied in this regard, and plenty of literature is available on the subject. It suggests that the addition of metallic nanoparticles, including gold, silver, platinum, palladium, copper, zinc, titanium, chromium, and boron, could overcome limitations in currently existing restorative materials [9]. Amongst these nanoparticles, silver (Ag) has been employed frequently in biomaterials to impart antimicrobial and antibacterial properties. It has been reported that silver imparts a positive effect on GIC, however, their mode of interaction has still not been fully understood [10]. A number of different techniques are also adapted to synthesize silver nanoparticles [11]. A more sustainable and biogenic approach seems to be a convenient method [12, 13]. The aim of the current investigation was to synthesize and characterize silver nanoparticles and then incorporate zinc oxide nanoparticles into commercially available resin-modified glass ionomer cement (RMGIC). The objective was to evaluate their chemical properties by Fourier transform infrared spectroscopy, micro-hardness, color stability, and their effect on the fluoride (F^-) release profile over a period of 14 days.

2 Materials and Methods

Resin-modified glass ionomer cement was procured from Fuji PLUS (Tokyo, Japan). Silver nitrate and chitosan (CH) were obtained from Riedel-de Haen GmbH and Chitoclear®, respectively. Sodium borohydride and acetic acid were supplied by Sigma Aldrich (St. Louis, MO,). Commercially available ZnO nanofillers (particle size < 100 nm; rod-like particles) were kindly supplied by EverZinc Chemicals.

2.1 Synthesis and Characterization of Silver Nanoparticles

The synthesis and characterization of silver nanoparticles (SNP) were reported earlier by Qasim et al. [10]. In brief, a 0.1% CH (w/v) solution was prepared by dissolving the required amount of CH into a 0.1 M acetic acid solution. Before the dropwise addition of acetic acid, CH was allowed to completely disperse in the distilled water. The reaction was conducted at 40 °C. In the next step, 3 mL of 0.1 M silver nitrate were added dropwise to the CH solution . The reaction was left stirring, and the temperature was raised to 90 °C for 2 h. This was followed by the addition of 4 mL of NaOH to the solution to complete the reduction of SNP. The change in color was taken as an indication of the formation of SNP [10].

2.2 Specimen Preparation

The experimental and control groups were prepared using a Perspex mold (diameter to thickness: 8 mm × 2 mm). The control specimens were prepared following the manufacturer's instructions and maintaining the powder to liquid ratio. Experimental specimens were prepared by incorporating either SNP (5 wt%) or ZnONP (5 wt%) individually or in a combination of SNP and ZnONP (5 wt %) at a ratio of 1:1 into RMGIC. After thorough mixing, the cement was carefully inserted into the mold using a thin cement spatula and pressed with the transparent mylar strip (Stripmat, Polydentia SA, CH-6805, Mezzovico, Switzerland), which was firmly attached to a transparent glass slide. Ultimate care was taken to avoid air bubbles being entrapped in the mixing and specimen preparation steps. Once the cement was placed , it set within 10 min. The set cement was carefully removed from the mold to prevent any further damage to the material.

2.3 Scanning Electron Microscopy

Specimens were examined through a scanning electron microscope (JEOL, JSM-5410LV, Tokyo, Japan). Each specimen was freshly prepared and stored for 24 h in the oven at 37 °C before being transferred to aluminum stub, which was covered by a carbon sticker and coated with gold in a sputter coater (Structure Probe, West Chester, PA) before being scanned and photographed at various magnifications (250×, 1500× and 4000×).

2.4 Fourier Transform Infrared Spectroscopy-

Fourier transform Infrared Spectroscopy (FTIR) spectra data was acquired on a Bruker Tensor 27 in attenuated total reflectance mode (ATR). Blank backgrounds were acquired prior to measuring each specimen. All specimens were crushed into powder and placed in close contact with the ATR crystal. Spectra were acquired in the wavenumber range of 4000 to 500 cm^{-1} operated at a resolution of 16 cm^{-1}. 32 scans were performed per specimen, and the results were reported as the means . The data was exported as a data point table and processed for peak analysis using OMNIC software (Thermo Scientific).

2.5 Nano Computerized Tomography

Computerized tomography of the specimens prepared for microhardness was measured on a Phoenix Nanotom (NanoCT, GR, USA). Scanning parameters were measured as: images acquired at a final isotropic resolution of 5-µm per voxel at 100 kV accelerating voltage and 100 µA current

with a 0.5 aluminum filter. Each specimen took 1.45 h for a single scan that resulted in 2000 images. Samples were scanned over 360° with a rotation step. The reconstruction process and data analysis for measuring the porosity percentage were performed using VGS Studio Max software (version 3.3). Porosity analysis was conducted by measuring the diameters of the pores using the porosity inclusion analysis of VGS Studio Max software. The data was exported as CVS files and plotted as frequency distribution graphs in GraphPad Prism (Version 8).

2.6 Microhardness

The test was performed on a digital microhardness tester that was equipped with a load cell of 50 g and measured for 20 s on the surface of the specimen with a Vickers diamond indentor (CV Instruments 400DAT/3) at room temperature (25 °C). The average value of 10 randomly selected points in each sample was taken into account for further analysis. The diagonal lengths of the indentations were measured with an objective lens at 40×. Microhardness in g μm^2 was calculated from the Eq. (1):

$$HV = 1854.4P/d^2 \quad (1)$$

Where HV is the Vickers Hardness, P is the load set in grams (g) and d is the diagonal's length in μm.

2.7 Color Stability

Three specimens were selected from each group (diameter: 8 ± 1 mm and thickness: 2 ± 1 mm). No polishing was conducted on the cured samples, which were stored at 25° ± 1 °C. The color measurement was conducted immediately after the curing within an hour (Day 0), 1, 4, 7, and 14 days using an Easy Shade spectrophotometer using 2° observation and D65 illumination (VITA Easyshade® V, GmbH & Co.KG Bad Säckingen, Germany). The software attached to the instrument calculated the CIELAB (Commission Internationale de léclairage) color values. The aim of the instrument is to detect the amount of light illuminated by an object and the amount of light reflected from it. The handheld device has a 5 mm measurement area that emits light using one halogen lamp. A background reading is performed by placing the probe tip in the calibration device built into the holder stand.

Each specimen is measured by placing the probe tip in the middle of the specimen at a 90° angle. Three random readings were taken from the top and bottom surfaces of the specimen. The instrument is comprised of an approximately uniform color space with color co-ordinates for white-black (L^*), redness-greenness (a^*) and yellowness-blueness (b^*). The mean L^*, a^* and b^* values were calculated at selected periods of 0, 1, 4, 7, and 14 days, while the color values at day 0 were considered the initial values as L_0, a_0, b_0. The color difference (ΔE) was calculated using Eq. (2):

$$\Delta E = \left[(L_0 - L)^2 + (a_0 - a)^2 + (b_0 - b)^2\right]^{0.5} \quad (2)$$

The clinical acceptability values were based on a value of ΔE 3.3. The operators were blinded at the time of analysing the specimens for microhardness, compressive strength, and color stability. This was done in order to eliminate the possibility of bias.

2.8 Fluoride Release

Experimental specimens were stored in distilled water (10 mL) and at selected periods of 2, 7, and 14 days, they were removed from the storage vials and transferred to a new vial containing fresh distilled water. At the end of the experimental period, the liquids were then analysed by high performance liquid chromatography (Prominence Shimadzu, Europe GmbH, Germany) with a UV–vis spectrometric detector to analyze and quantify the release of F^- from the commercial and experimental RMGICs used in this study. An IC-A_3 column was used with the mobile phase containing 4-hydroxy benzoic acid, Bis, Tris, Boric acid, phosphate (PO_4^{3-}), Fluoride (F^-), Chlorie (Cl^-), Bromide (Br^-), Nitrate (NO_3^-) and sulphate (SO_4^{2-}). The data shown in the study only reports on the fluoride ion.

2.9 Statistical Analysis

Unless otherwise stated, all experiments were conducted in triplicate. GraphPad Prism Software (Version 8) was used for performing the statistical analysis.

3 Results

The SEM micrographs are presented in Fig. 1. The control specimen shows a smooth morphology, with higher magnification showing the distribution of particles. The addition of 5% SNP retains the morphology with a homogenous particle distribution, as can be seen in the inset image at a higher magnification (Fig. 1b). Incorporation of both SNP and ZnONP resulted in a cracked surface with the appearance of pores (Fig. 1c). The specimens with ZnONP at 5% (Fig. 1d) nevertheless displayed a rough surface when compared with the control and the neat SNP specimens. Porosities were evident in both lower and higher magnification images.

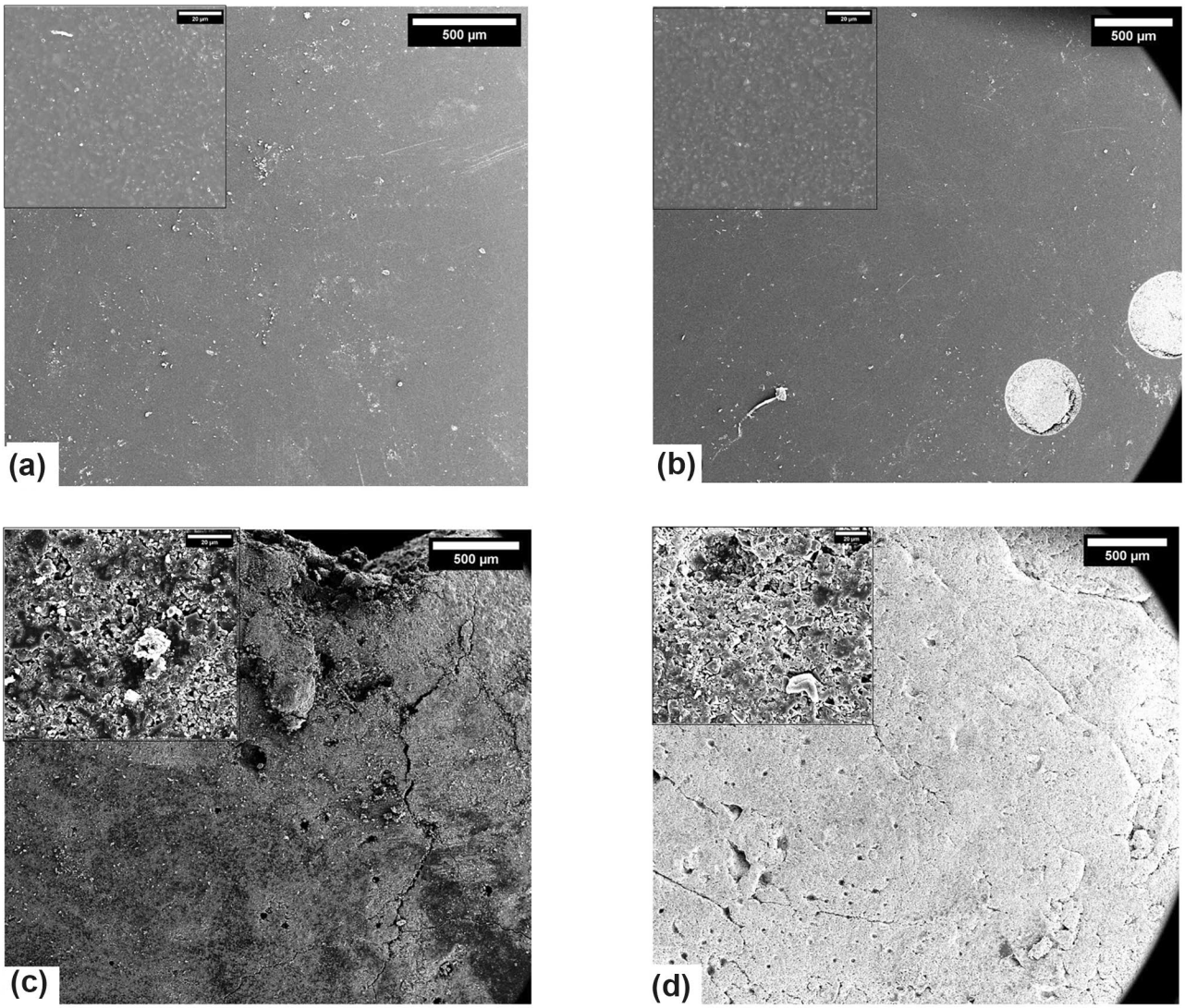

Fig. 1 Scanning electron micrographs of (a) Control (b) GIC with 5 wt % SNP (c) 5 wt % SNP and ZnONP (d) 5 wt% ZnONP, All images are scaled at 500 µm and have inset images at higher magnification scaled at 20 µm

The FTIR spectra for all specimens are shown in Fig. 2a and b. The broad band located at 3351 cm^{-1} is assigned to the stretching vibration of the O-H group. This could be due to the water within the cement or the -OH group present in poly(HEMA). Another marginal band adjacent to a band at 2951 cm^{-1} is assigned to the C-H stretching vibration of the polyacrylic acid. The presence of SiO_2 and phosphate is observed as an asymmetric stretching vibration at 1028 and 960 cm^{-1} respectively (Fig. 2a). The FTIR spectral data revealed a high intensity band at 1716 cm^{-1}, which is indicative of the symmetric stretch of the carboxylic group -C=O band and the peak at 1634 cm^{-1} indicated the methacrylate C=C bond (C=C str). This peak was more pronounced as compared to additional low-intensity bands at 1454, 1408, 1321 and1299 cm^{-1} (Fig. 2b). The shoulder observed at 1161 cm^{-1} may be assigned to the C-O stretching of the carboxylic group, which corresponds to both, tartatric and poly(acrylic) acids. A peak that is peculiar to the spectral profile of 5% ZnONP is the one at 1577 cm^{-1} that is attributed to the carboxylate salt formed (C=O str of COOM). Moreover, the low intensity peaks at 1454 and 1408 cm^{-1} became more pronounced. These double bands are attributed to the asymmetric and symmetric -COO^- stretch bands, respectively. The appearance of the peak at 1255 cm^{-1} in experimental specimens is atributes to acid C-O stretch.

Typical nano-computerized tomography images and porosity analysis are presented in Fig. 3. The scans revealed pores that were heterogeneous in all specimens within the core of the materials and equally distributed. Scans of specimens containing 5% SNP+5% ZnONP and 5% ZnONP

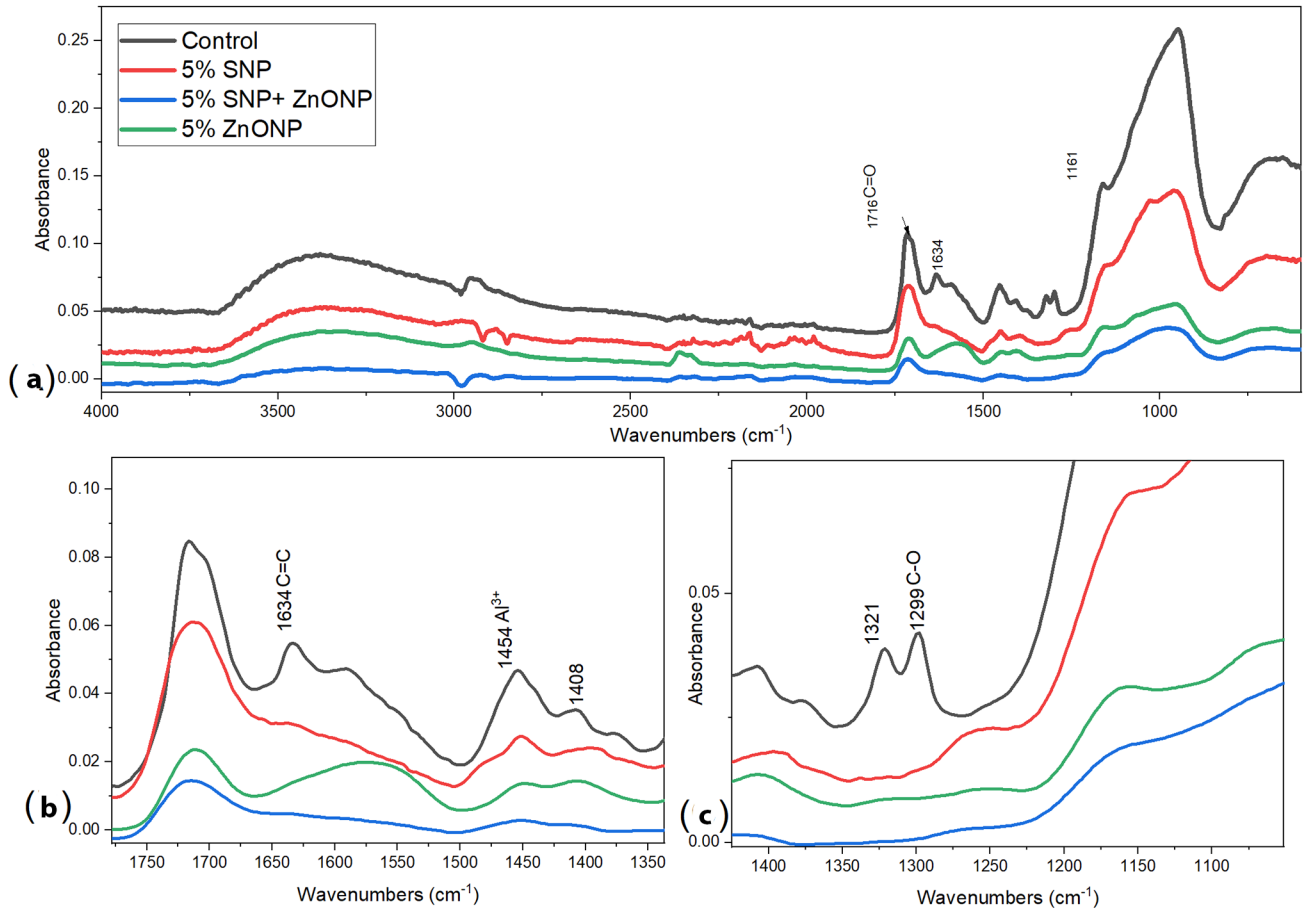

Fig. 2 FTIR spectra of (a) complete spectra ranging from 4000 to 500 cm^{-1} (b and c) Finger print region showing the alterations, peak intensity profile, peak shifts in C = O, C-O, COO, acquired in ATR mode

demonstrated significant cracks and considerably larger pores. The porosity analysis (Fig. 4) furthermore visualizes the frequency distribution of the cracks. The control specimen showed a spike in pores of 30 µm. 5% SNP showed considerably lesspore distribution. With pores having a concentration of 20 µm. 5% SNP + 5% ZnONP and 5% ZnONP impregnated RMGIC improved the pore diameter with a larger distribution of particles (20–100 µm). Porosity analysis is represented as a frequency distribution, as represented in Fig. 4a to d.

Results from the Vickers micro-hardness (HV) measurements are presented in Fig. 5. A significant difference in hardness is noted between the control and the specimen containing 5% SNP + 5% ZnONP. The combined NPs (5% SNP + 5% ZnONP) enriched specimens had the lowest mean hardness values. After 14 days of storage, the hardness of the control specimen (27.22 ± 0.99) is comparable to that of the specimen doped with 5% ZnONP (24.89 ± 1.33). The specimens doped with 5% SNP showed a lowering in the microhardness values with time (1 to 14 days).

The released Fluoride ions from the test specimens were detected by the HPLC. These can be seen in a typical chromatogram, as shown in Fig. 6. Different peaks with their respective retention times can be observed. The results from the color difference (ΔE) and F^- release studies are represented in (Fig. 7a and b). The ΔE of the control specimens remained constant at 2.4 ± 1.47 after 14 days, while the values were amplified to a range between 19.78 ± 2.65 and 21.88 ± 6.71 for experimental samples. In terms of the F^- release (mg / L), the control, 5% SNP, and 5% SNP + 5% ZnONP specimens at day 2 showed values of 3.84 ± 0.88, 5.15 ± 0.36 and 3.87 ± 0.04, respectively. The maximum values were recorded for 5% SNP + 5% ZnONP specimens. The F^- analysis revealed that the control and 5% SNP + 5% ZnONP incorporated samples had a slower release on day 2, and increased thereafter on day 7. On the other hand, 5% ZnONP doped specimens, showed a burst in the F^- release initially and slowed down on day 7.

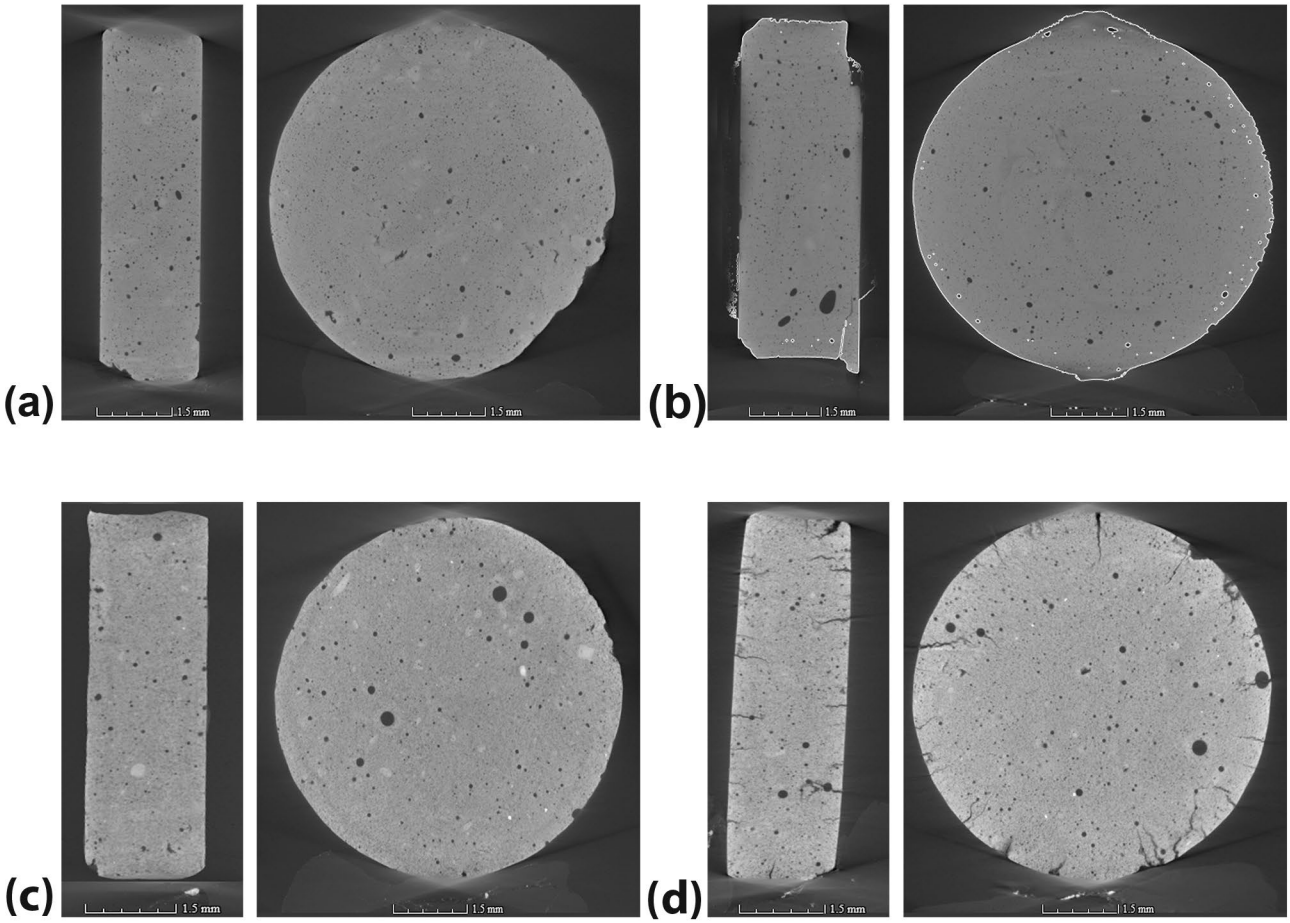

Fig. 3 Nanocomputerized tomography of (a) Control ((b) GIC with 5 wt % SNP (c) 5 wt % SNP and ZnONP (d) 5 wt% ZnONP, Cross-sectional and longitudinal images scaled at 1.5 µm. Images display pores distribution in the examined specimen

4 Discussion

The addition of metallic nanoparticles to the physiochemical and biological properties of dental restorative materials has been an area of special interest. The possibility of therapeutic achievement correlated with nanoparticles depends mainly on the inherent properties of these biomaterials, such as their surface area, chemical reactivity, and biological activity [14]. Although studies in the past have reported nanoparticles like aluminum oxide (Al_2O_3), zirconium oxide (ZrO_2), titanium dioxide (TiO_2) [15, 16] and ZnONP [17]. However, these studies have only reported the addition of a single type of nanoparticle in each group and investigated properties like flexural and compressive strength [15, 16]. Whereas, the current investigation reports on the combined effect of two different nanoparticles in comparison to their addition alone. The SNP particles synthesized in our previous study were adapted for the current investigation [10]. In the current study, SNP was added to the liquid component while mixing , and ZnONP was mixed with the powder before mixing. Three experimental groups were tested, with the control being the unmodified RMGIC. The addition of SNP alone did not significantly alter the surface. Since it was devoid of any visible surface crazing or voids, whereas its combination with ZnONP and ZnONP alone altered the ultrastructural morphology with the formation of cracks and pores. The presence of voids or porosities has been reported earlier as well [18]. They are known to act as stress raisers (stress concentrations), which eventually cause mechanical failure of the restorative materials during their clinical life cycle [16]. Moreover, it has been speculated that they can initiate fracture and are the main cause of cohesive failure as well [19].

The NanoCT investigation revealed greater insights into the pores and pore size frequency distribution within the specimens. These porosities could be attributed to the hand mixing that was conducted to prepare the experimental specimens [10]. Earlier, similar investigations were conducted on the addition of SNP (1–2 wt%) and ZnO (0 to 4 wt%) as compared to the present study, where the

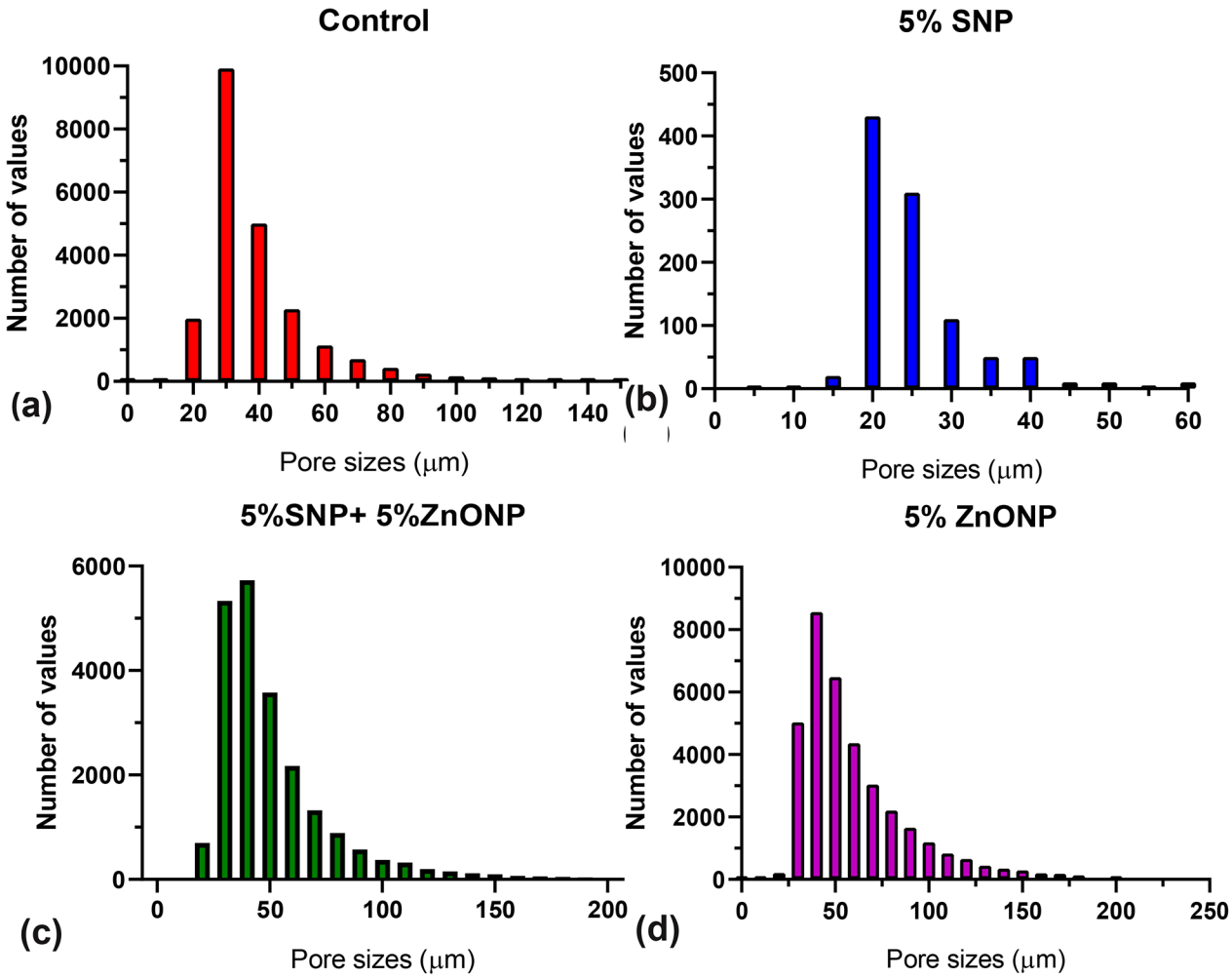

Fig. 4 Frequency distribution graphs to analyze pore size (μm) conducted by Nanocompterized tomography on (a) Control, (b) 5% SNP, (c) 5% SNP + 5% ZnONP, (d) 5% ZnONP

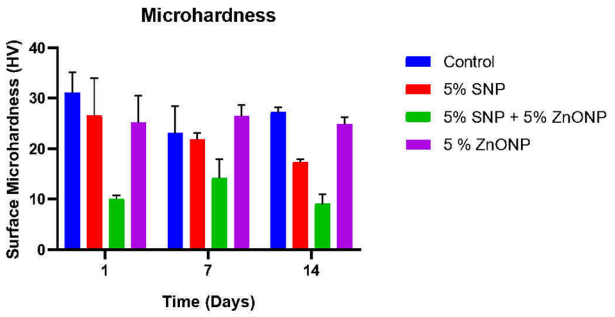

Fig. 5 Microhardness of (a) Control and experimental (b) GIC with 5 wt % SNP (c) 5 wt % SNP and ZnONP (d) 5 wt% ZnONP, Values shown are mean ± SD where (n = 3), A significant (*) difference was noted in between 5% SNP + 5%ZnONP and 5%ZnONP

nanoparticle concentration increased to 5 wt%. These investigators reported that the addition of 2 wt% nanoparticles imparted superior antimicrobial activity without altering the F^- release. Gjorgievska et al. reported that there was a reduction in the presence of microscopic voids with the addition of Al_2O_3, ZrO_2 and TiO_2 in high viscosity conventional GIC [16]. However, the voids were analysed on the surface using SEM analysis, whereas the current investigations utilized Nano CT for bulk pore analysis. thereby, showing that the pores (voids) were not only present on the surface but also in the core material. In another study, a significantly higher ZnO concentration from 0 to 15 wt % was impregnated into glass ionomer cement [20]. This high concentration intensified the viscosity of the cement , making the fabrication of specimens difficult. An increase in the viscosity was observed in the experimental specimens, which could be attributed to the significant improvement of the surface area by nanoparticles. The authors speculate that

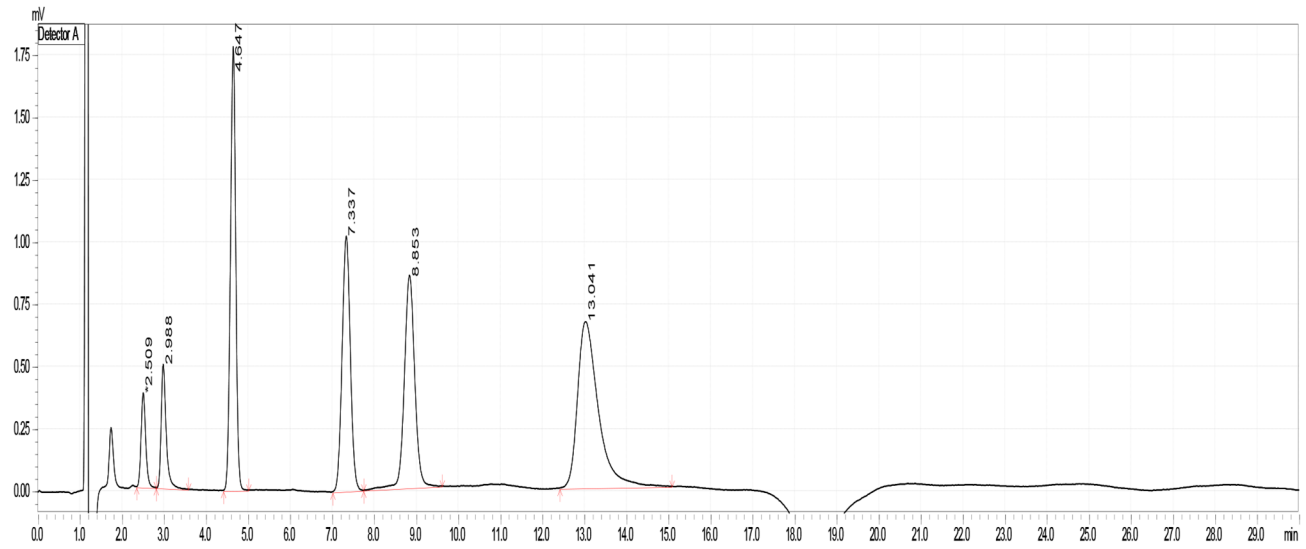

Fig. 6 A typical HPLC chromatogram of experimental specimen with 5% ZnONP following 2 days of immersion in distilled water

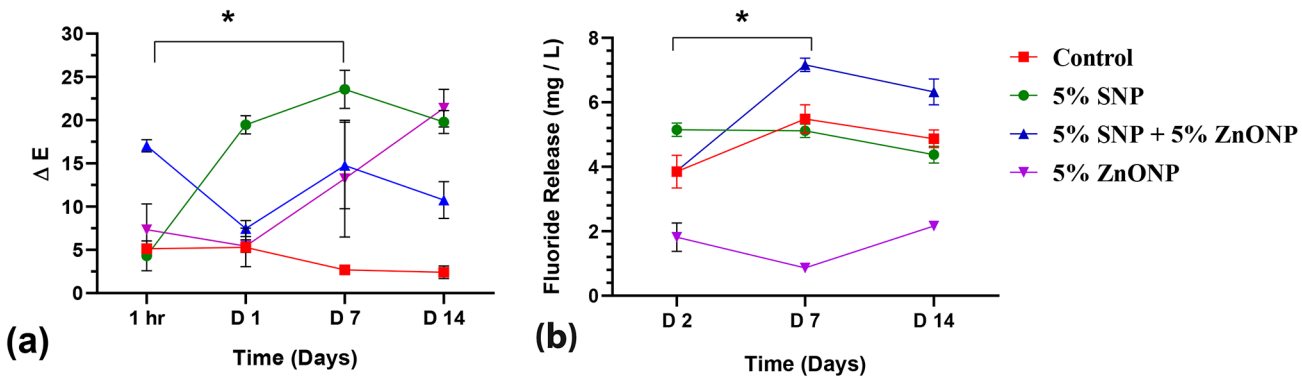

Fig. 7 (a) Color stability and (b) Fluoride release analysis of Control, GIC with 5 wt % SNP, 5 wt % SNP and ZnONP and 5 wt% ZnONP. Values shown are mean ± SD (n = 3). A statistically significant difference was noted in between values acquired on Day 1 and 7 in between control and 5% SNP only. Similarly for fluoride release a significant difference was noted for values acquired on day 2 and 7 in between control and 5%SNP + 5%ZnONP

the increment in viscosity could be correlated to the cement liquid being insufficient to wet the added ZnONP.

A spectroscopic investigation conducted in the past after the incorporation of nanoparticles revealed that the peaks at 1570 and 1420 cm^{-1}, showed higher intensities. Peaks pertaining to methacrylate groups (C = C) were noted in the control specimen at 1299 and 1321 cm^{-1}, which were reduced in intensity in the experimental groups. The progress of the acid-base reaction is observed by the appearance of the peak 1577 cm^{-1}, which has been assigned to the growth of the carboxylate salt peak (C = O stretching of the COO^{-}) [21]. A spectroscopic investigation performed by Young reported that polyacrylate salts with mono or divalent counterions usually have symmetric and asymmetric COO^{-} stretch bands at around 1420 and 1540 cm^{-1}[22]. With respect to the interaction of SNP with RMGIC, it has been reported that an electrostatic stabilization occurs due to steric and electrostatic repulsions at polyelectrolyte adsorptions on a colloidally positively charged particle surface [23]. Pavia et al., investigated the incorporation of silver in GIC and speculated that nanoparticles should be dispersed in the GIC matrix as the cement completes the setting reaction [23].

Results from the microhardness test revealed some interesting findings. A decrease in the surface microhardness was noted when the nanoparticles were combined. Individual additions to the specimens did not decrease the hardness as much as when both particles were added together. Reports from the literature on the effect of nanoparticle inclusion on hardness, flexural and shear bond strength have shown variations. A decrease in the mechanical properties has been reported, and this was attributed to the less compact surface or larger quantities of pores [20]. In another study,

El-Wassefy et al., incorporated SNP into conventional GIC [24]. Results from their study showed that SNP had an insignificant effect on the mechanical properties and a noticeable influence on the coloration. The results of the current study were in agreement with El-Wassefy et al., whereby the addition of SNP and SNP + ZnONP significantly reduced the mechanical properties. Moreover, a significant alteration in the color was also observed. Color changes of RMGICs associated with the addition of SNP present a significant limitation, especially when they are incorporated into biomaterials intended for use in aesthetic areas. Nonetheless, incorporation of SNP to GICs at various concentrations was found to have significant differences in color change when compared to non-reinforced GICs [10]. The incorporation of ZnONP into RMGICs was expected to provide more light to the material and, as a result, neutralize the darkness caused by the addition of SNP. However, this was not observed during the present investigation, and the color stability values for the 5% SNP and 5% ZnO-NP incorporated RMGICs were considered unacceptable.

Fluoride (F^-) release studies conducted in the current investigation using high performance liquid chromatography have also been reported earlier [25]. However, the identified ions were different from our study (data not shown). Only F- ion was reported in the current investigation. According to the investigation conducted by Verbeeck et al. on F- release from RMGIC's, they reported that the release of this ion is the result of two processes occurring simultaneously [26]. The first process is short term initial elution, occurring instantly, and then terminating after some time. Also called the early wash-out stage [27]. Whereas, the second phase is associated with prolonged and more slowly occurring release, which is responsible for the long term release of F- [26]. Also called the sustained diffusion stage [27]. Furthermore, Glass ionomer cements, whether resin modified or not, behave as cation permselective membranes, therefore the release is governed by the maturation time, which is the time elapsed between the start of the acid base setting reaction and the moment that the set cement comes into contact with an aqueous solution [26, 28]. In terms of F- ion released, Basso et al.[29] compared F- ions released from different dental materials. They showed that the highest amounts were among the RMGIC group, with a high burst release initially and stabilizing afterwards. A similar result was also noted by Dziuk and co-workers [30]. In the current investigation, interpretations of the release profile can be speculated to display an initial burst release that then declines. This was similar to the results observed in this study for the three groups tested. The presence of SNP in this study had no effect on the amount of F- ions released, either positively or negatively. The discrepancy in the release of F from the observed specimens in the current study could also be attributed to several extrinsic factors. Similarly, Paschoal et al. (2011) found a higher F- release by RMGICs compared to conventional GICs [31]. The highest number of F- ions detected in this study was for the 5% SNP and 5% ZnO-NP incorporated RMGIC groups. This amount of F ions released is advantageous; however, as previously stated, it comes at the expense of microhardness and color stability. This limitation may be improved by the incorporation of a smaller concentration of ZnONP in order to maintain the high amount of F- ions released with an improvement in the surface microhardness and color stability. Nevertheless,, Hellwig et al. reported in an in-vitro study that a concentration of 0.01 ppm F- is sufficient to facilitate remineralization [32].

5 Conclusion

The addition of SNP and ZnONP alone and in combination t with resin modified glass ionomer cement revealed significant reductions in the levels of surface microhardness due to the presence of pores within the that were distributed uniformly throughout the bulk specimen. Color stability for specimens reinforced with SNP and ZnONP together was stable, and the fluoride release was also enhanced. Overall, we conclude that the combined addition of two different nanoparticles is beneficial for resin modified glass ionomer cements and has the potential to lead to significant improvements in other physiochemical, biological, and mechanical properties allowing it to used in clinical conditions. Future work should now be undertaken to analyze the ion release from these reinforced cements.

Acknowledgements The authors would like to acknowledge SRUL 01/14 and Dental Biomaterials research lab at the Kuwait University. Electron Microscopy Unit at the Faculty of Medicine, Kuwait University and Kuwait University Nanotechnology Research Facility (GE 01/17).

Funding No funding was acquired for this project.

Declarations

Conflict of Interest The authors declare that there are no conflicts of interest or relationship, financial or otherwise associated with this study.

Ethical Approval Not Applicable.

Consent to Participate Not Applicable.

Consent for Publication Not Applicable.

References

1. J.F. Roberts, N. Attari, M. Sherriff, Br. Dent. J. **198**(7), 427–431 (2005)
2. T.P. Croll, J.W. Nicholson, Pediatr. Dent. **24**(5), 423–429 (2002)
3. M. Łępicka, M. Rodziewicz, M. Kawalec, K. Nowicka, Y. Tsybrii, K.J. Kurzydłowski, J. Mech. Behav. Biomedical Mater. **133**, 105324 (2022)
4. D.W. Berzins, S. Abey, M.C. Costache, C.A. Wilkie, H.W. Roberts, J. Dent. Res. **89**(1), 82–86 (2010)
5. M.A. Cattani-Lorente, V. Dupuis, J. Payan, F. Moya, J.M. Meyer, Dent. Mater **15**(1), 71–78 (1999)
6. A. Valanezhad, T. Odatsu, K. Udoh, T. Shiraishi, T. Sawase, I. Watanabe, J. Mater. Sci. Mater. Med. **27**(1), 3 (2016)
7. A. Komori, H. Ishikawa, Angle Orthod **67**(3), 189–196 (1997)
8. J.W. Nicholson, B. Czarnecka, Dent. Mater **24**(12), 1702–1708 (2008)
9. H. Moradpoor, M. Safaei, H.R. Mozaffari, R. Sharifi, M.M. Imani, A. Golshah, N. Bashardoust, RSC Adv. **11**(34), 21189–21206 (2021)
10. S.S.B. Qasim, D. Ali, M.S. Soliman, G.-G. Zafiropoulos, Mater. Res. Express **8**(8), 085401 (2021)
11. S.H. Lee, B.H. Jun, Int J Mol Sci. 20(4) (2019)
12. M. Darroudi, M.B. Ahmad, A.H. Abdullah, N.A. Ibrahim, K. Shameli, Int. J. Mol. Sci. **11**(10), 3898–3905 (2010)
13. A.P.V. Ferreyra Maillard, P.R. Dalmasso, B.A. Lopez, de Mishima, A. Hollmann, Colloids Surf. B Biointerfaces **171**, 320–326 (2018)
14. A.A. Balhaddad, A.A. Kansara, D. Hidan, M.D. Weir, H.H.K. Xu, M.A.S. Melo, Bioact Mater. **4**(1), 43–55 (2019)
15. E. Gjorgievska, J.W. Nicholson, D. Gabrić, Z.A. Guclu, I. Miletić, N.J. Coleman, Materials. **13**(2), 276 (2020)
16. E. Gjorgievska, G. Van Tendeloo, J.W. Nicholson, N.J. Coleman, I.J. Slipper, S. Booth, Microscopy and Microanalysis. **21**(2), 392–406 (2015)
17. P. Garcia, M.F.B. Cardia, R.S. Francisconi, L.N. Dovigo, D.M.P. Spolidorio, A.N. de Souza, Rastelli, A.C. Botta, Microsc Res. Tech. **80**(5), 456–461 (2017)
18. F.M. Abed, S.B. Kotha, H. AlShukairi, F.N. Almotawah, R.A. Alabdulaly, S.K. Mallineni, Front. Bioeng. Biotechnol. **10**, 816652 (2022)
19. S.E. Elsaka, I.M. Hamouda, M.V. Swain, J. Dent. **39**(9), 589–598 (2011)
20. P. Agarwal, R. Nayak, P.N. Upadhya, K. Ginjupalli, L. Gupta, Materials Today: Proceedings. **5**(8, Part 3), 16065–16072 (2018)
21. A. Falsafi, S.B. Mitra, J.D. Oxman, T.T. Ton, H.T. Bui, Dent. Mater. **30**(6), 632–643 (2014)
22. A.M. Young, Biomaterials. **23**(15), 3289–3295 (2002)
23. L. Paiva, T.K.S. Fidalgo, L.P. da Costa, L.C. Maia, L. Balan, K. Anselme, L. Ploux, R.M.S.M. Thiré, J. Dentistry **69**, 102–109 (2018)
24. N.A. El-Wassefy, R.H. El-Mahdy, N.R. El-Kholany, J. Esthet Restor. Dent. **30**(2), 146–152 (2018)
25. A. Agha, S. Parker, E.K. Parkinson, M. Patel, Dent. Mater. **37**(10), 1542–1552 (2021)
26. R.M.H. Verbeeck, E.A.P. De Maeyer, L.A.M. Marks, R.J.G. De Moor, A.M.J.C. De Witte, L.M. Trimpeneers, Biomaterials. **19**(6), 509–519 (1998)
27. S.K. Sidhu, J.W. Nicholson, J Funct Biomater. 7(3) (2016)
28. H.J.J. Roeykens, R.M.H. Verbeeck, *and M. LC. The permeability of some resin-modified glass-ionomer cements. in Third Congress of the European Academy of Paediatric Dentistry* (Brugge, 1996)
29. G.R. Basso, Á Della Bona, D.L. Gobbi, D. Cecchetti, Brazilian Dent. J. **22**, 355–358 (2011)
30. Y. Dziuk, S. Chhatwani, S.C. Mohlhenrich, S. Tulka, E.A. Naumova, G. Danesh, PLoS One **16**(2), e0247716 (2021)
31. M.A. Paschoal, C.V. Gurgel, D. Rios, A.C. Magalhaes, M.A. Buzalaf, M.A. Machado, Braz Dent. J. **22**(4), 275–279 (2011)
32. E. Hellwig, A. Lussi, Caries Research. **35(suppl 1)** (suppl. 1), 57–59 (2001)